



## Modeling and Simulation of Respiratory System for Acute Respiratory Distress Syndrome (ARDS) Associated with COVID-19

Mohamed Elnoby Awad<sup>\*1</sup>, Ahmed M. El-Garhy<sup>2</sup>, Mohamed A. Eldosoky<sup>1</sup>, Ahmed M. Soliman<sup>1</sup>

<sup>1</sup>Biomedical Engineering Department, Faculty of Engineering, Helwan University, Cairo, Egypt.

\* mohamedelnoby@yahoo.com

mohamed\_eldesouky@h-eng.helwan.edu.eg

ahmed\_soliman05@h-eng.helwan.edu.eg

<sup>2</sup>Communications and Electronics Engineering Department, Faculty of Engineering, Helwan University, Cairo, Egypt.

agarhy2003@yahoo.co.in

### ABSTRACT

The respiratory system is one of the complicated systems in the human body. In this paper, the mathematical model for the respiratory system was proposed based on the electro-acoustic bio-impedance analysis with huge number of equations. Further, the behavior of each generation from 24 generations of the respiratory system can be analyzed separately. Furthermore, the pressure with ventilated frequency from 1-1200 min<sup>-1</sup> at any generation can be predicted and calculated. The proposed mathematical model was validated by comparison the results with the published results. The simulated results for ARDS disease are presented. Also, the comparison between normal case (healthy) and ARDS diseased case is presented. The proposed mathematical model with huge number of equations is implemented by Matlab program package. This proposed mathematical model can be used as a reversed problem solution to detect and diagnose the medical situation of the respiratory system for patients especially patients associated with COVID-19.

**Keywords-** Electro-Acoustic Bioimpedance, Modeling and Simulation, Respiratory System, Covid-19, ARDS.

### I. INTRODUCTION

The human respiratory system is one of the major and complex systems in human body. The lung is divided to conducting, transitional and respiratory zones [1]. The conducting zone is consisting of nose, pharynx, larynx, trachea and bronchial tree [2]. The conducting zone functions are tracking the air to and from the lung, filtering the air from dusts and pathogens, warming and humidifying the air which flows to the lung. The respiratory zone is consisting of bronchioles, alveolar ducts, clusters of alveoli and alveoli sacs. The main function of the respiratory zone is the gas exchange between the red blood cells and the air. The gas exchange is the processing to deliver the oxygen from the lung to the body tissues and eliminate the carbon dioxide from blood stream to the lung [3].

Acute respiratory distress syndrome (ARDS) and chronic obstructive pulmonary disorder (COPD) are major and popular diseases which can affect the respiratory system [4]. ARDS is a respiratory disease characterizing by rapid onset of prevalent inflammation in the lung. The fluids are accumulated in the alveoli. These fluids prevent filling the lung with sufficient air. Therefore, ARDS has symptoms such as shortage of the breathing, high frequency of the breathing, and bluish color to the skin. ARDS impairs the ability of lung to exchange oxygen and carbon dioxide. There are many causes can lead to ARDS such as trauma, sepsis, aspiration pancreatitis, and pneumonia [5].

A novel coronavirus (nCoV) or COVID-19 is a new strain of Coronaviruses (CoV) family. COVID-19 has not been previously identified in humans. The infection of COVID-19 speeded in most countries of the world and became pandemic as the world health organization (WHO) declared [6]. COVID-19 is a one of Coronaviruses (CoV) which are a large family of viruses that cause many diseases. The diseases of Coronaviruses are ranging from the common cold to more severe diseases such as Severe Acute Respiratory Syndrome (SARS-CoV) and Middle East Respiratory Syndrome (MERS-CoV). Coronaviruses are transmitted between animals and people.. The common signs of Coronaviruses' infection include cough, respiratory symptoms, breathing difficulties, fever, and shortness of breath. Further, it can cause pneumonia, ARDS, blood clotting, kidney failure, and even death [7]. The COVID-19 patients are classified into two types of patients [8]. Type 1 of patients, they have severe hypoxemia, relatively normal respiratory mechanics, high value of gas volume of the lung, and minimal ability of lung recruitment. Type 2 of patients, they have severe hypoxemia, low compliance, low value of gas volume of the lung, and high ability of lung recruitment of lung. Type 2 of patients is indicated as ARDS patients. Computed tomography (CT) scan can

be used to distinguish between type 1 of patients (non ARDS patients) and type 2 of patients (ARDS patients). Recently, COVID-19 is the most popular virus leading to ARDS disease. About 20-30% of patients associated with COVID-19 are admitted to the intensive care units (ICU) associated with severe hypoxemia and deterioration of the compliance indicating severe ARDS [9].

The respiratory system is very complex especially the lung which consisting of complex network of branching compliant tubes spanning a wide range of scales and flow regimes. According to the complexity of respiratory system, the analysis of respiratory system to obtain its mechanical properties is required for diagnosis and the treatment of the pulmonary diseases. The modeling of respiratory system can resolve many problems in behaviour of lung and chest. Therefore, the modeling of respiratory system can provide the interpretations of different pulmonary variables such as pressure, volume, and airflow for different cases, diseases, and assisting in patient specific treatment planning and optimization.

The bioimpedance is a common terminology used widely in different applications of biomedical engineering [10, 11]. The bioimpedance analysis is used in the modeling by simulating any vital tissue in form of electrical parameters such as: inductance ( $L$ ), Capacitance ( $C$ ), and resistance ( $R$ ). Also, this model is called  $RLC$  electrical model.

In this paper, the mathematical model for the respiratory system is proposed based on the electro-acoustic bio-impedance analysis with huge number of equations. Further, the behaviour of each generation from 24 generations of the lung can be analyzed separately as in many cases some regions of respiratory system can be affected in different manners. Furthermore, the pressure with ventilated frequency from  $1-1200 \text{ min}^{-1}$  at any generation can be calculated. The proposed mathematical model based on the mechanical parameters of respiratory system is represented as electrical circuit. The electrical circuit is represented by passive component inductance ( $L$ ), Capacitance ( $C$ ), and resistance ( $R$ ). The relations among the total lung impedance (TLI), the ventilation frequency ( $f$ ), inductance ( $L$ ), Capacitance ( $C$ ), and resistance ( $R$ ) of the system are presented. At specific input pressure, the mathematical model can provide the accurate calculations for the pressure value at each generation of the 24 generations of the lung and at given ventilation frequency. The proposed mathematical model was validated by comparison the results with the published results [12]. The simulated results for ARDS disease are presented. Also, the comparison between normal case (healthy) and ARDS disease is presented. The proposed mathematical model with huge number of equations is implemented by Matlab program package. The proposed mathematical model is important and essential for assisting the physicians to predict and diagnose the type 2 of COVID-19 patients and provide the suitable support of ventilations for them.

## A. LITERATURE REVIEW

Paul Harper et al [13] developed a model of acoustical properties of reparatory tract over tracheal sound frequency range 100-3000 Hz. The tract of respiratory was represented as transmission line acoustical analogy. This representation was varied with the area of cross section, yielding of walls, and branching of dichotomous. The developed model can provide the location in frequency of natural acoustic resonances of components or the entire of respiratory tract. The prediction of tracheal spectral peaks from the speech sounds was presented by the model. This prediction was detected at the mouth and the trachea. This model provided the relationship between the tracheal sounds and the anatomy of the tract of respiratory.

M. Rozanek et al [12] introduced the electro-acoustic analogy model for respiratory system. The model can provide the acoustic parameters of respiratory system from the electrical system. The model was based on the passive electrical components resistance ( $R$ ), inductance ( $L$ ), and capacitance ( $C$ ). The respiratory system was represented in this model based on the Weibel model [14]. The Weibel model represented the lung as 24 generations with symmetric for both lungs. The model presented the TLI and the pressure at the generations with limited frequencies. Really, the impedance of lung at different frequencies including low and high frequencies are required to study and analyse different respiratory diseases. They assumed that low frequencies are used during artificial lung ventilation (ALV) but actually the high frequency ventilation is also used in the ventilation especially in some ARDS cases in neonates. The other disadvantage of this paper is the model dividing into the compartments and the parameters of each compartment computing independently. Further, the disability to determine a specific pressure at any generation of the respiratory system with actually ventilation frequency range  $1 - 1200 \text{ min}^{-1}$  ( $1/60 - 5 \text{ Hz}$ ) is also disadvantage of this paper.

Surajit Bagchi et al [15] proposed the electrical model of respiratory system to detect and identify bronchitis and emphysema diseases which are the ventilation common diseases. These two diseases are some of types of chronic obstructive pulmonary disease (COPD). The developed model was represented the respiratory system as analogy electrical components. The transfer function and the stability of the system were analyzed and compared for healthy and COPD. The model in this paper had many disadvantages. Different assumptions of the model were too simplified and were not realistic. The two lungs with its all branches and generations were considered in the mathematical model as a one unit. Also, the effect of any disease at any specific generation cannot be indicated or estimated. Further, the flow paths of the air in the bronchi were assumed in the model as collected again. This assumption was not matched with the physiological functions of the respiratory system.

Shumit Saha et al [16] developed a model of upper airway for snoring sounds generation. This model called subject-specific acoustic model. The objective of this model was investigating the anatomy of upper airway such as the length, the thickness of wall, and the area of the cross section. The proposed model was validated as the intensity of sound and resonant frequency of the model were compared with the measured of recorded snoring sounds achieved during sleep for 20 individual males. According to the obtained results, the only factor affecting the snoring sound intensity was the narrowing of the upper airway. Also, the snoring frequencies were inversely correlation with the length of upper airway. The results showed that the analysis of snoring sound during the sleep can predict the anatomy of upper airway.

Parya Aghasafari et al [17] proposed 3D model for healthy lung captured by Magnetic Resonance Imaging (MRI). This 3D model was analysed by computational fluid dynamic. The pressure applied on the wall of lung is essential for setting up and protecting lung strategy. Therefore, the curve fitting was obtained to estimate the relation among the pressure, time of breathing, the cross section, and the generation number. This relation provided the necessary information required during the mechanical ventilation. From the obtained results, the exponential and polynomial pressure functions were the most accurate for normal breathing and mechanical ventilation, respectively. The good correlation of pressure location curves was predicted from the comparison between the computational fluid dynamic and the results obtained from this study.

A. V. Bogomolov et al [18] presented the mathematical model of the sound absorption by lung. The modeling was simulated the respiratory system using acoustics. The respiratory mechanics was studied by the propagation of acoustics in the respiratory system. The main objective of the developed model was the determination of the resonant frequency of the respiratory tract. This resonant frequency is essential to increase the vital capacity of lung. High intensity acoustic signal was applied with respiratory system. The resonant frequency can be measured using impedance characteristic prior the stimulation. The stimulation was achieved by the scanning tonal sound at  $\pm 3$  dB which was the maximum absorption coefficient value. The results showed the increasing of the vital capacity of the lung according to the acoustic stimulation. Also, the area of cross section was the only factor proportional with the vital capacity and the resonant frequency of respiratory system.

Lorenzo Aliboni et al [19] introduced the simulation of bronchial airway acoustics for both healthy and asthmatic patients. Acoustical pressure propagation analytical model was applied to CT images of lung for both healthy and severe asthmatic patients. System response to input acoustical pressure (1 Pa) at 200 and 600 Hz was evaluated in terms of distribution of acoustical pressure, acoustical radial wall velocity, and acoustical impedance. The results appeared that acoustic parameters were sensitive to the variation of airways caused by asthma pathology at fraction residual capacity (FRC) and total lung capacity (TLC).

Based on the literature analysis, the accurate modeling of the respiratory system is essential to study and analyse the pulmonary parameters of the respiratory system. Further, the modeling is important for assisting the physicians to diagnose the pulmonary diseases of patients and provide the suitable support of ventilations for patients. Therefore, the proposed mathematical model based on the electro-acoustic bio-impedance analysis for the respiratory system is represented with huge number of equations. The proposed model can provide more accurate results and a solution to overcome the disadvantages obtained from other models. The accurate results obtained by the proposed mathematical model are based on the huge number of equations which described the respiratory system. All equations are calculated without any assumptions; therefore, the accurate results compared to other methods are obtained. Also, the model provides accurate analysis of the pulmonary parameters for each generation from 24 generations of the respiratory system. Furthermore, the pressure with a wide range of the ventilation frequency from 1-1200  $\text{min}^{-1}$  at any generation can be calculated.

## II. METHODOLOGY

In this paper, the proposed model is an electro-acoustic based model. The electro-acoustic model imitates the acoustic properties of the respiratory system with electrical components. The proposed model is based on the Weibel model. The Weibel model is a morphological and anatomical model of the respiratory system [14]. As shown in Fig. 1, the Weibel model represented the lung as 24 generations (from G0 to G23) with symmetric for both lungs. Every generation has  $2^n$  of airways, where  $n$  is the generation number. Therefore, the total number of airways in Weibel model is 16,777,215. Also, the Trachea is represented as generation number 0 (G0), from generation number 1 to 16 is represented of the conducting zone, and from generation number 17 to 23 is represented of transitional and respiratory zone. The Alveoli start appearing from the generation number 17; therefore, the process of gas exchanges is beginning from this generation [20].

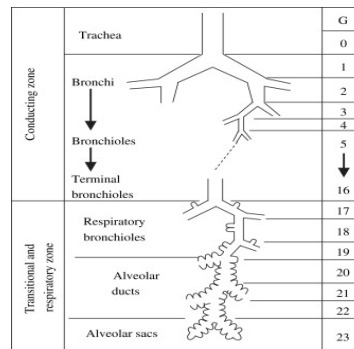


Fig. 1: Weibel model [14].

Table 1: Model Airways geometrical dimensions with average adult lung volume 4800 ml at about  $\frac{3}{4}$  maximal inflation.

Generation Number (n)	Number Of Airways In The Generation	Diameter Of Airway Inside Generation (d)	Length Of Airway In The Generation (l)
0	1	1.8	12
1	2	1.22	4.76
2	4	0.83	1.9
3	8	0.56	2.76
4	16	0.45	1.27
5	32	0.35	1.07
6	64	0.28	0.90
7	128	0.23	0.76
8	256	0.186	0.64
9	512	0.154	0.54
10	1024	0.13	0.46
11	2048	0.109	0.39
12	4096	0.095	0.33
13	8192	0.082	0.27
14	16384	0.074	0.23
15	32768	0.066	0.20
16	65536	0.060	0.165
17	131072	0.054	0.141
18	262144	0.050	0.117
19	524288	0.047	0.099
20	1048576	0.045	0.083
21	2097152	0.043	0.070
22	4194304	0.041	0.059
23	8388608	0.041	0.050

Mansoura University, Mansoura, Egypt

Based on Weibel model, the geometrical dimensions of the respiratory system model with average adult lung with volume 4800 ml at about  $\frac{3}{4}$  maximal inflation including lengths and diameters of airways, and the number of airways in each generation are represented in Table 1 [14]. Every airway in the same generation has the same length and diameter. The geometrical dimensions of the respiratory system are used in our proposed mathematical model as acoustic system.

The electro-acoustic model is represented the acoustic properties as electrical components [12]. The mathematical model is proposed to calculate and achieve the relations among the total lung impedance (TLI), the variation of the ventilated frequency (f), resistance (R), inductance (L) and capacitance (C) of the system. Every airway in the respiratory system is considered as lumped electrical circuit model with passive component R, L and C as illustrated in Fig. 2.

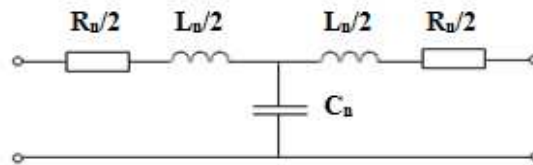


Fig. 2: Lumped electrical circuit model.

The electro-acoustic equations are represented based on lumped electrical circuit model. Further, the acoustical inductance ( $m_a$ ), acoustical compliance ( $C_a$ ), and acoustical resistance ( $r_a$ ) for every airway in the respiratory system are calculated as represented in equations 1, 2, and 3 [12]:

$$m_a = \frac{\rho_0 l}{S} \quad (1)$$

$$C_a = \frac{V}{\rho_0 c_0^2} \quad (2)$$

$$r_a = \frac{8\mu l}{\pi R_t^4} \quad (3)$$

Where,  $\rho_0$  is the air density and equal  $1.225 \text{ kg/m}^3$  at standard temperature pressure (STP),  $l$  is the airway length,  $S$  is the airway cross-section area,  $V$  is the volume,  $C_0$  is the propagation velocity,  $\mu$  is the air viscosity and equal  $1.81 \cdot 10^{-5} \text{ kg/(m.s)}$  (STP), and  $R_t$  is the airway diameter. For every airway in the respiratory system, the lumped circuit parameters are represented according to the electro-acoustic analogy as shown in Fig. 3.

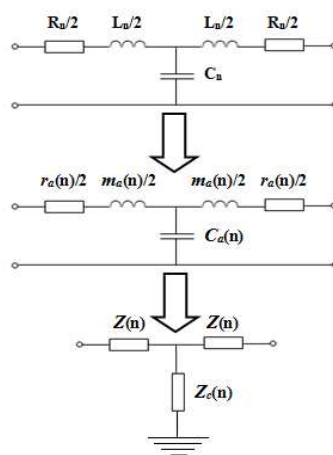


Fig. 3: Electro-acoustic analogy.

The impedance of each inductance ( $L$ ) and capacitance ( $C$ ) components in every respiratory generation  $X_L(n)$  and  $X_C(n)$  can be computed as represented in equation (4) and (5), respectively.

$$X_L(n) = 2 \pi f L(n) \quad (4)$$

$$X_C(n) = \frac{1}{2 \pi f C(n)} \quad (5)$$



Mansoura University, Mansoura, Egypt

Where,  $f$  is the ventilated frequency, and  $n$  is the generation number. According to Fig. 3, the final impedances of lumped circuit according to the electro-acoustic analogy for every respiratory generation are represented:

$$Z_C(n) = X_C(n) \quad (6)$$

$$Z(n) = R(n) + \frac{X_L(n)}{2} \quad (7)$$

The final proposed electrical model of respiratory system is illustrated in Fig. 4.

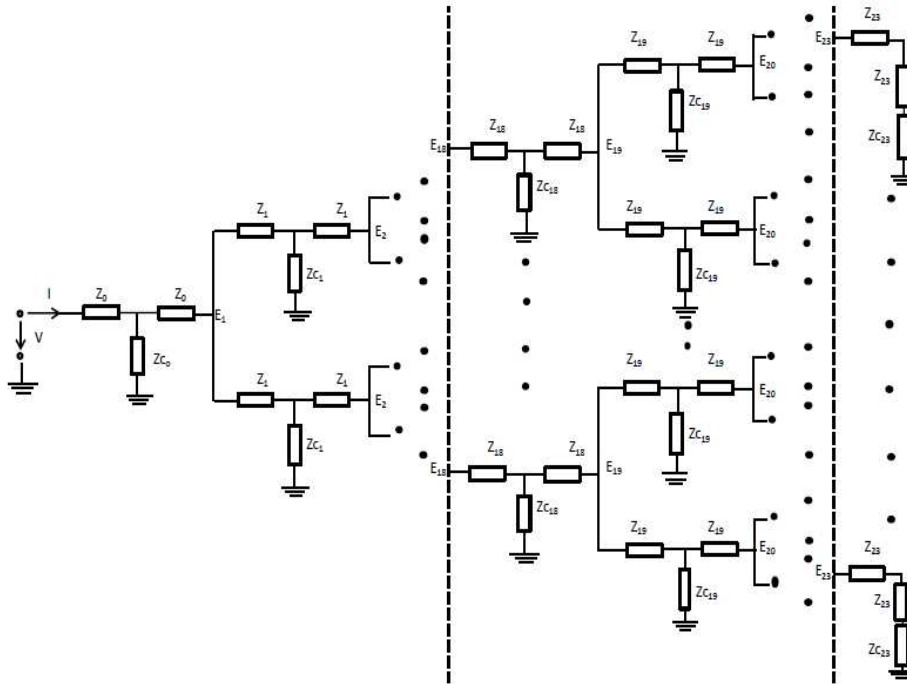


Fig. 4: The Proposed electrical model of the respiratory system.

The proposed electrical model of the respiratory system is very complicated as shown in Fig. 4. This electrical model consists of 16,777,215 lumped circuits with 67,108,859 passive components. Therefore, the special method is required to solve a huge circuit and number of equations. However, we developed a new method to calculate these equations. Also, the Matlab program was built to solve these equations and calculate the TLI with the ability to calculate the respiratory parameters at each node of the respiratory system. In the proposed model, the solution of reverse problem is used to calculate the total TLI and the respiratory parameters at each node of the respiratory system. Every equivalent lumped impedance can be computed separately for selected frequency as follows:

$$E(23) = \frac{2Z(23) + Z_C(23)}{2} \quad (8)$$

The nodal impedances  $E(22)$ ,  $E(21)$ ,  $E(20)$ ...to  $E(1)$  can be derived and computed respectively from the generation number ( $n$ ) 22 to 1 from the equation number (9) as following:

$$E(n) = \frac{1}{2} \frac{(E(n+1) + Z(n)) * Z_C(n)}{(E(n+1) + Z(n)) + Z_C(n)} + Z(n) \quad (9)$$

Then the TLI for the selected frequency is calculated as following:

$$TLI = \frac{(E(1) + Z(0)) * Z_C(0)}{E(1) + Z(0) + Z_C(0)} + Z(0) \quad (10)$$

Using Equations (8), (9), and (10), the TLI and the respiratory parameters at each node of the respiratory system can be calculated at specific values of  $R$ ,  $L$ ,  $C$  and  $f$ . The Matlab program was built to solve and calculate the equations for the wide range of frequencies ( $1-1200 \text{ min}^{-1}$ ).

According to the electro-acoustic analogy, the distribution of the pressure along the generations will be presented as a percentage of the input pressure and will be represented by the nodal voltage further it will be implemented and

calculated by matlab software according the distribution of impedances which actually varies according to the type of disease and its severity.

### III. RESULTS AND DISCUSSION

The proposed mathematical model with huge number of equations is implemented by Matlab program package. The Matlab program was built to solve these equations and calculate the TLI and the respiratory parameters at each node of the respiratory system.

The results are divided to two parts. The first part presents the validation of the proposed mathematical model by comparing the simulated results from the implemented Matlab program with published results [12]. The second part presents the simulation of pressure detection for any point of respiratory system for normal and ARDS cases.

#### A. THE VALIDATION OF THE PRESENTED METHODOLOGY AND SOFTWARE PROGRAM

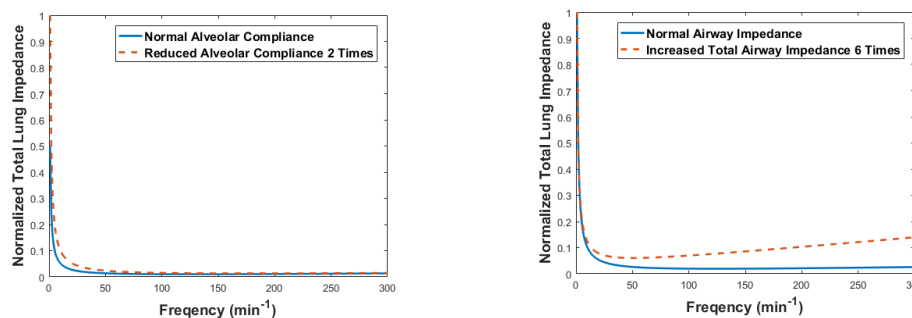


Fig. 5: The relation between normalized TLI and ventilated frequency for: (a) Normal alveolar compliance and reduced alveolar compliance by two times, (b) Normal total airway impedance and increased total airway impedance 6 times.

In Fig. 5, the relations between normalized TLI and ventilated frequencies are represented. As shown in Fig. 5(a), the normal alveolar compliance and reduced alveolar compliance by two times are simulated. The TLI has a significant change in the low frequency ventilation (LFV). But, for the high frequency ventilation (HFV), it has very little change due to reduce the alveolar compliance by 2 times but in Fig. 5(b) the normal airway impedance and increased airway impedance by 6 times are simulated. The TLI has significant change in HFV and very little change in LFV due to increasing the airway pressure by 6 times.

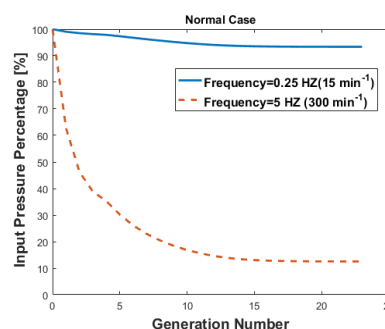


Fig. 6: The relations between the percentage of the input pressure and the number of generations at two ventilated frequencies 0.25 Hz (15 min<sup>-1</sup>) and 5 Hz (300 min<sup>-1</sup>) for both normal alveolar compliance and airway resistance.

In Fig. 6, the relations between the percentage of the input pressure and the number of generations at two ventilated frequencies 0.25 Hz (15 min<sup>-1</sup>) and 5 Hz (300 min<sup>-1</sup>) for normal alveolar compliance and airway resistance are presented. The change of frequency affects on the pressure distribution along the model of respiratory system generation as above 90% of input pressure appeared in the last generations during LFV (0.25 Hz) and around 10% appeared in last generations during HFV (5 Hz).

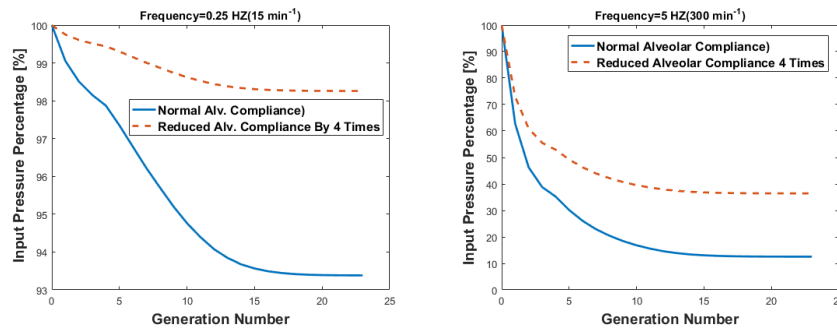


Fig. 7: The relations between the percentage of the input pressure and the number of generations at: (a) 0.25 Hz ( $15 \text{ min}^{-1}$ ) ventilated frequency for normal alveolar compliance and reduced alveolar compliance by 4 times, (b) 5 Hz ( $300 \text{ min}^{-1}$ ) ventilated frequency for normal alveolar compliance and reduced alveolar compliance by 4 times.

In Fig. 7, the relations between the percentage of the input pressure and the number of generations at 0.25 Hz ( $15 \text{ min}^{-1}$ ) and 5 Hz ( $300 \text{ min}^{-1}$ ) ventilated frequencies for normal alveolar compliance and reduced alveolar compliance by 4 times are represented. As shown in Fig. 7(a), the reduced alveolar compliance by 4 times during LFV at 0.25 Hz can cause slight increase of the pressure along the generations but in Fig. 7(b) it causes during HFV at 5 Hz increase the pressure along the generations by around 4 times.

From the above, all presented simulations and results were compared and verified with published results [12]

## B. THE SIMULATION OF PRESSURE DETECTION FOR ANY POINT OF RESPIRATORY SYSTEM FOR NORMAL AND ARDS CASES

The aim of this presented simulation is studying and analyzing the behaviour of the complete system and every localized diseased part in respiratory system separately and its effects on the complete system.

The pressure distribution in normal and ARDS cases according to their severity with wide range of ventilated frequency [ $1/60 - 20\text{Hz}$ ] ( $1-1200 \text{ min}^{-1}$ ) are simulated. Also, the distinguishing from the output signals of the normal and ARDS cases and their severity and validation of some explanation and practice experience in medicine is presented. Furthermore, in mechanical ventilation, it is a helpful tool for selecting proper ventilation parameters such as pressure, frequency, and tidal volume.

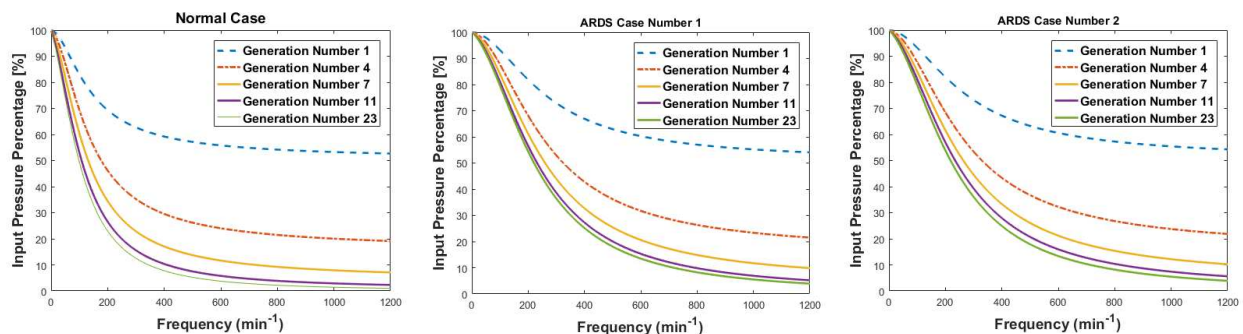


Fig. 8: The relations between the percentage of the input pressure and the wide range of ventilated frequency [ $1/60 - 20\text{Hz}$ ] ( $1-1200 \text{ min}^{-1}$ ) for the selected generations 1, 4, 7, 11 and 23 for: (a) Normal case, (b) case number 1 (c) ARDS case number 2.

Firstly, the model according to the presented methodology was simulated at normal compliance for all generations. As shown in Fig. 8(a), the relations between the percentage of the input pressure and the wide range of ventilated frequency [ $1/60 - 20\text{Hz}$ ] ( $1-1200 \text{ min}^{-1}$ ) for the selected generations 1, 4, 7, 11 and 23 are represented.

Secondly, the model was simulated for ARDS case number 1 as the compliances for transitional and respiratory zone (Generation 17 to 23) were deteriorated and decreased by 4 times. For this case, Fig. 8(b) presented the relations between the percentage of the input pressure and the wide range of ventilated frequency [ $1/60 - 20\text{Hz}$ ] ( $1-1200 \text{ min}^{-1}$ ) for the selected generations 1, 4, 7, 11 and 23, respectively.

Thirdly, the model was simulated for ARDS case number 2 as the compliances for transitional and respiratory zone (Generation 17 to 23) were deteriorated and decreased by 4 times and the airway resistance increased by 2 times. The assumption of the increasing of airway resistance is due to the deterioration of these generations resulted from edema and accumulated fluids. For this case, Fig. 8(c) presented ARDS case 2 as the relations between the percentage of the input pressure and the wide range of ventilated frequency [ $1/60 - 20\text{Hz}$ ] ( $1-1200 \text{ min}^{-1}$ ) for the selected generations 1, 4, 7, 11 and 23, respectively.



Finally, different simulations for normal and ARDS case are simulated as the compliances of transitional and respiratory zone (Generation 17 to 23) were deteriorated and decreased by 4 times. For these simulations, Figs 9 and 10 presented the relations between the percentage of the input pressure and the wide range of ventilated frequency [1/60 – 20Hz] (1-1200 min<sup>-1</sup>) for the selected generations 1, 7, and 23, respectively.

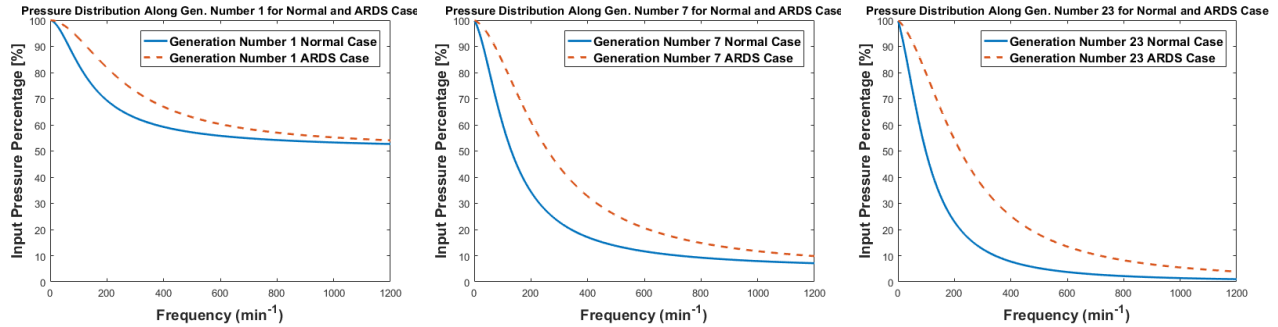


Fig. 9: The relations between the percentage of the input pressure and the wide range of ventilated frequency [1/60 – 20Hz] (1-1200 min<sup>-1</sup>) for normal and ARDS case for the selected generation number (a) 1, (b) 7, (C) 23

As shown in Fig. 9(a), the pressure distribution for normal and ARDS case at generation number 1 is represented. The pressure for ARDS case along the generation number 1 is greater than in the normal case at the same input pressure. The pressure distribution is decreasing for both normal and ARDS cases with increasing the ventilated frequency. The maximum pressure difference between the normal and ARDS case is around 12.69% as appeared in 175 min<sup>-1</sup> ventilated frequency. Also, the pressure difference at 1200 min<sup>-1</sup> ventilated frequency is approximately 1.39%. Moreover, the minimum pressure percentage for the normal case is 52.69% and found at ventilated 1200 min<sup>-1</sup> frequency. The studied ARDS case has the minimum pressure percentage 54.08% and found at ventilated 1200 min<sup>-1</sup> frequency.

As shown in Fig. 9(b), the pressure distribution for normal and ARDS case at generation number 7 is represented. The pressure for ARDS case along the generation number 7 is greater than in the normal case at the same input pressure. The pressure distribution is decreasing for both normal and ARDS cases with increasing the ventilated frequency. The maximum pressure difference between the normal and ARDS case is around 27.61% as appeared in 162 min<sup>-1</sup> ventilated frequency. Also, the pressure difference at 1200 min<sup>-1</sup> ventilated frequency is approximately 2.73%. Moreover, the minimum pressure percentage for the normal case is 7.11% and found at ventilated 1200 min<sup>-1</sup> frequency. The studied ARDS case has the minimum pressure percentage 9.84% and found at ventilated 1200 min<sup>-1</sup> frequency.

As shown in Fig. 9(c), the pressure distribution for normal and ARDS case at generation number 23 is represented. The pressure for ARDS case along the generation number 23 is greater than in the normal case at the same input pressure. The pressure distribution is decreasing for both normal and ARDS cases with increasing the ventilated frequency. The maximum pressure difference between the normal and ARDS case is around 33.33% as appeared in 149 min<sup>-1</sup> ventilated frequency. Also, the pressure difference at 1200 min<sup>-1</sup> ventilated frequency is approximately 2.91%. Moreover, the minimum pressure percentage for the normal case is 1.01% and found at ventilated 1200 min<sup>-1</sup> frequency. The studied ARDS case has the minimum pressure percentage 3.92% and found at ventilated 1200 min<sup>-1</sup> frequency.

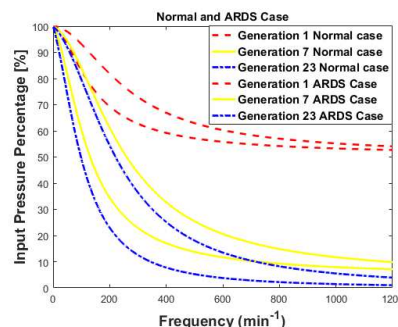


Fig. 10: The relations between the percentage of the input pressure and the wide range of ventilated frequency [1/60 – 20Hz] (1-1200 min<sup>-1</sup>) for the selected generations 1, 7, and 23 for normal and ARDS case.

In Fig. 10, the simulation for both normal and ARDS cases for the selected generations 1, 7 and 23 was presented. Some of medical explanations can be concluded from the analysis of Figs 8, 9 and 10 as following:

- Pressure distribution for ARDS cases along the generations and ventilated frequencies is always greater than in the normal case at the same input pressure.
- The more increasing frequency, the less pressure inside the generation.
- At any selected ventilated frequency, the pressure is decreasing with increasing the generation number.
- The pressure difference between any two generations for the same case is increasing with the increasing the ventilated frequency as it reaches to the maximum difference at  $1200 \text{ min}^{-1}$  ventilated frequency.
- The pressure difference between normal and ARDS case at the same generation is increasing with increasing the ventilated frequency to specific value depends on the generation number. This specific ventilated frequency is decreasing and shifted to the left with increasing the generation number.
- At last value of ventilated frequency  $1200 \text{ min}^{-1}$ , the pressure difference between normal and ARDS case is increasing with increasing the generation number.
- The Pressure distribution difference between normal and ARDS case increasing with increasing generation number.
- The pressure difference between upper airways is more significant than the distal ones.
- No significant change in pressure distribution in ARDS cases 1 and 2 as the ARDS affects mainly lung compliance.

#### IV. CONCLUSION

Covid-19 is one of the most critical viruses nowadays as it spreads rapidly and considered as a pandemic. It affects the reparatory system and cause rapid deterioration in some patients like who have chronic diseases.

The mathematical model for the respiratory system is proposed based on the electro-acoustic bio-impedance analysis. Huge number of equations were derived and calculated to solve this complicated model and implemented by Matlab program package. All equations are calculated without any assumptions; therefore, the accurate results compared to other methods are obtained. The proposed model presented methodology and software program were validated and be able to study and discuss different diseases of respiratory system such as COPD, Asthma, Pneumonia, and ARDS with their different severity. ARDS case was studied, discussed and compared with normal case, the result was presented. The TLI and prediction of the pressure distribution in all generations of respiratory system with different ventilation frequencies are presented.

The proposed model is helpful tool and can be one of reasons in selecting the ventilator modes, waveform pattern and ventilators parameters according to the kind of disease and its severity. In reverse problems, it can be a tool in auto diagnose of respiratory system diseases.

#### REFERENCES

- [1] R. L. Maynard, S. Pearce, B. Nemery, P. D. Wagner, B. Cooper, and J. E. Cotes, “Cotes’ Lung Function,” 7<sup>th</sup> ed., Wiley Blackwell, 2020.
- [2] P. Slinger, “Principles and Practice of Anesthesia for Thoracic Surgery,” Springer Nature Switzerland AG, 2019.
- [3] S. P. Bhatt, “Cardiac Considerations in Chronic Lung Disease”, Humana Press, 2020.
- [4] M. Matthay, R. Zemans, G. Zimmerman, Y. Arabi, J. Beitler, A. Mercat, M. Herridge, A. Randolph, and C. Calfee, “Acute Respiratory Distress Syndrome”, *Nature Reviews Disease Primers*, vol. 5, 2019.
- [5] S. Rayees, I. Din, G. Singh, and F. A. Malik, “Chronic Lung Diseases”, Springer Nature, 2020.
- [6] The World Health Organization website. [Online]. Available: <http://www.who.int>
- [7] Y. Wang, Y. Wang, Y. Chen, and Q. Qin, “Unique Epidemiological and Clinical Features of The Emerging 2019 Novel Coronavirus Pneumonia (COVID-19) Implicate Special Control Measures”, *Journal of Medical Virology*, Vol. 92, pp.568-576, 2020.
- [8] L. Gattinoni, D. Chiumello, and S. Rossi, “COVID-19 pneumonia: ARDS or not?” *Critical Care*, vol. 24, 2020.
- [9] H. Okada, S. Yoshida, A. Hara, S. Ogura and H. Tomita, “Vascular Endothelial Injury Exacerbates Coronavirus Disease 2019: The Role of Endothelial Glycocalyx Protection”, *Microcirculation*, pp.1-7, 2020.



- 
- [10] A Y. Shash, M. Eldosoky, and M. Elwakad, "Detection of stenosis in blood vessel by using bio-impedance analysis", 2018 35<sup>th</sup> National Radio Science Conference (NRSC), 2018.
- [11] R. Abdelbaset, M. Eldosoky, and M. El-Wakad, "The Effect of Heart Pulsatile on The Measurement of Artery Bioimpedance", *Journal of Electrical Bioimpedance*, vol. 8, pp.101-106, 2019.
- [12] M. Rozanek, Z. Horakova and K. Roubik, "Electro-Acoustic Analogy and Its Use for Modelling of Biological Systems", 6<sup>th</sup> International Conference on Electrical and Power Engineering, Romania, 2010. [http://www.epe.tuiasi.ro/2010/pdf/EMC\\_2010.pdf](http://www.epe.tuiasi.ro/2010/pdf/EMC_2010.pdf)
- [13] P. Harper, S. Kraman, H. Pasterkamp and G. Wodicka, "An Acoustic Model of the Respiratory Tract", *IEEE Transactions on Biomedical Engineering*, vol. 48, no. 5, pp. 543-550, 2001.
- [14] E. Weibel, A. Cournand and D. Richards, *Morphometry of the Human Lung*, Berlin: Springer Berlin, 1963.
- [15] S. Bagchi and M. Chattopadhyay, "Electrical Modeling of Respiratory System and Identification of Two Common COPD Diseases Through Stability Analysis Technique", *IEEE International Conference on Advanced Communication Control and Computing Technologies (ICACCCT)*, India, 2012.
- [16] S. Saha, T. Bradley, M. Taheri, Z. Moussavi and A. Yadollahi, "A Subject-Specific Acoustic Model of the Upper Airway for Snoring Sounds Generation", *Scientific Reports*, vol. 6, no. 1, 2016.
- [17] P. Aghasafari, I. Ibrahim and R. Pidaparti, "Modeling Pressure Relationships of Inspired Air into the Human Lung Bifurcations Through Simulations", *International Journal for Computational Methods in Engineering Science and Mechanics*, vol. 19, no. 2, pp. 69-81, 2018.
- [18] A. Bogomolov, S. Dragan and G. Erofeev, "Mathematical Model of Sound Absorption by Lungs with Acoustic Stimulation of the Respiratory System", *Doklady Biochemistry and Biophysics*, vol. 487, no. 1, pp. 247-250, 2019.
- [19] L. Aliboni, F. Pennati, T. Royston, J. Woods and A. Aliverti, "Simulation of Bronchial Airway Acoustics in Healthy and Asthmatic Subjects", *PLOS ONE*, vol. 15, no. 2, p. e0228603, 2020.
- [20] R. Ghorbani, A. Blomberg, and F. Schmidt, "Modeling Pulmonary Gas Exchange and Single-Exhalation Profiles of Carbon Monoxide", *Frontiers in Physiology*, vol. 9, 2018.